

Electronic Supplemental Information:

The Diversity of Aluminum-Based Drinking Water Treatment Residuals for Use in Environmental Remediation

Samuel M. Wallace,^a Yuchi Zhang,^a Lang Zhou,^b Qing Ma,^c William E. Guise,^c Nancy D. Denslow,^d Jean-Claude Bonzongo,^b and Jean-François Gaillard*^a

^a Department of Civil and Environmental Engineering, Northwestern University, 2145 Sheridan Road, Evanston, IL 60208, USA. E-mail: jf-gaillard@northwestern.edu

^b Engineering School of Sustainable Infrastructure and Environment, Department of Environmental Engineering Sciences, University of Florida, PO Box 116450, Gainesville, FL 32611, USA.

^c DND-CAT Synchrotron Research Center, Northwestern University, 9700 South Cass Avenue, Argonne, IL 60439, USA.

^d Departments of Physiological Sciences and of Biochemistry and Molecular Biology and Center for Environmental and Human Toxicology, University of Florida, University of Florida, Gainesville, FL 32610, USA.

A Supplemental Data

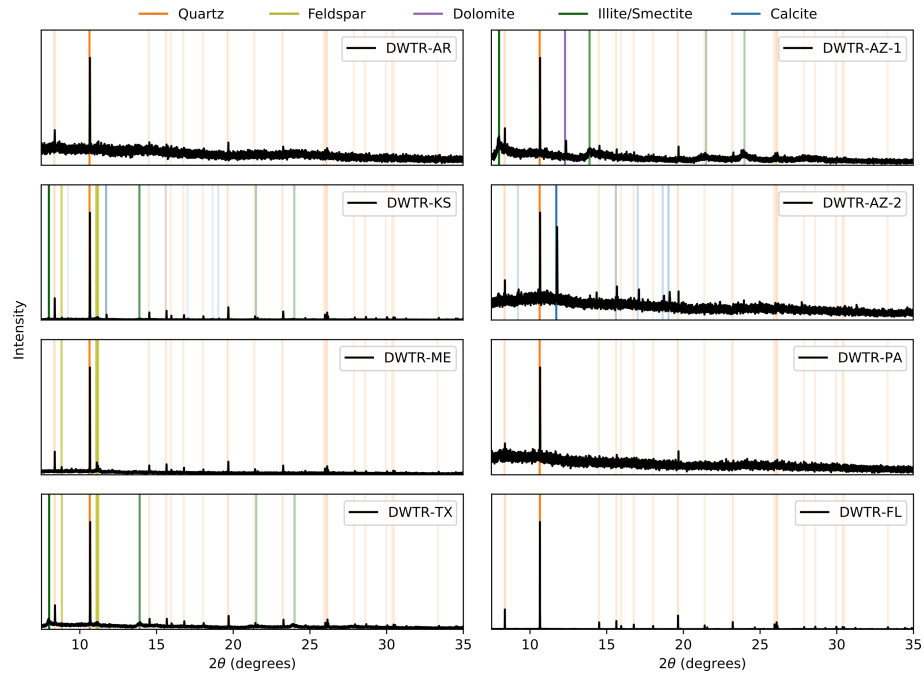


Figure 1: Synchrotron-source X-ray diffraction patterns for other DWTR samples not the focus of this study. Data were collected using the same methodology described in the Material and Methods' section. The same phases identified in the main DWTR samples are identified in these other samples in varying combinations, which include clay (illite and/or smectite), feldspar (albite and microcline), carbonate minerals (calcite and dolomite), and quartz. Again, not present in these samples are crystalline iron oxides or aluminum oxides.

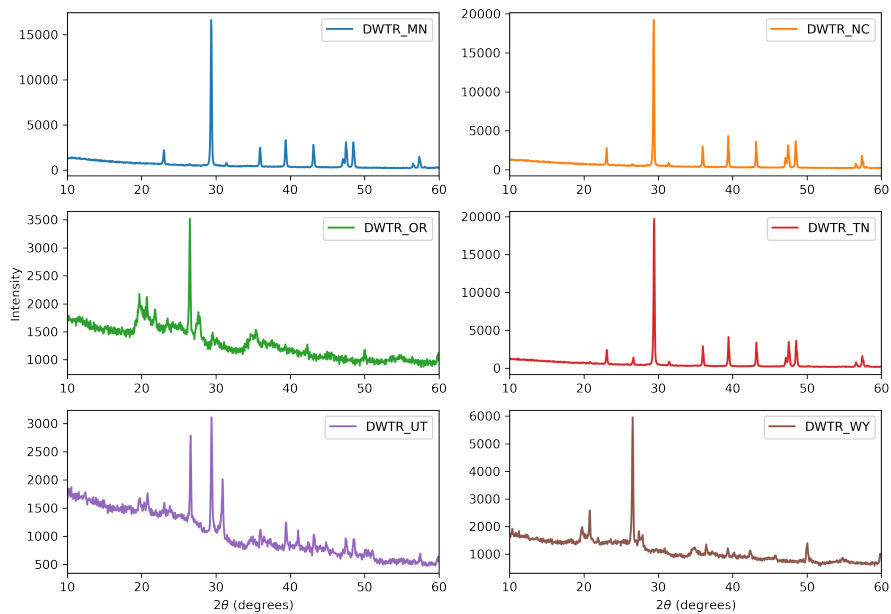


Figure 2: Laboratory-source X-ray diffraction patterns for the six DWTR samples. Data were collected using a Rigaku Ultima IV with a Cu X-ray source at the Jerome B. Cohen X-Ray Diffraction Facility at Northwestern University, Evanston, IL. Patterns for highly-crystalline components, such as quartz and calcite, remain easily identifiable, though peaks for feldspars are indistinct, and the diffraction peak for dolomite in DWTR-WY is not observed in the laboratory-source XRD.

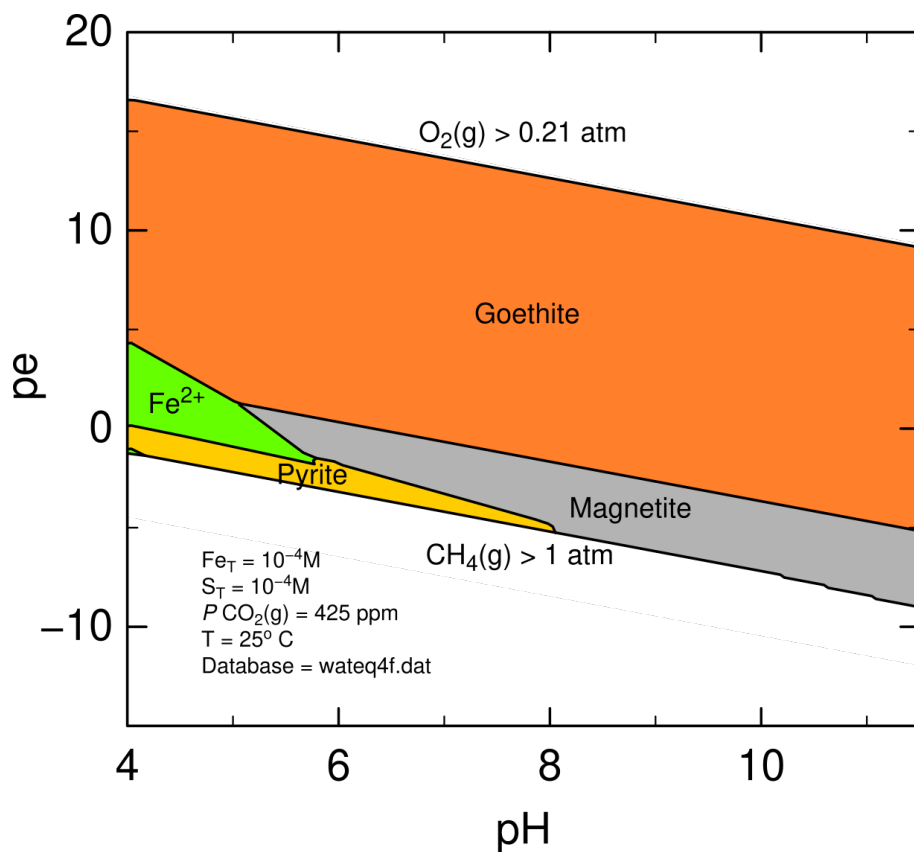


Figure 3: Pourbaix diagram showing stable iron phases in solution. Calculations were performed and plotted using Phreeplot software¹ and WATEQ4F thermodynamic database². Calculations are based on 100 μM total Mn, 100 μM total S, equilibrium with 425 ppm atmospheric CO_2 , and 25°C temperature. Hematite is not included in the calculations here to emphasize iron phases that are more easily formed through surface water processes.

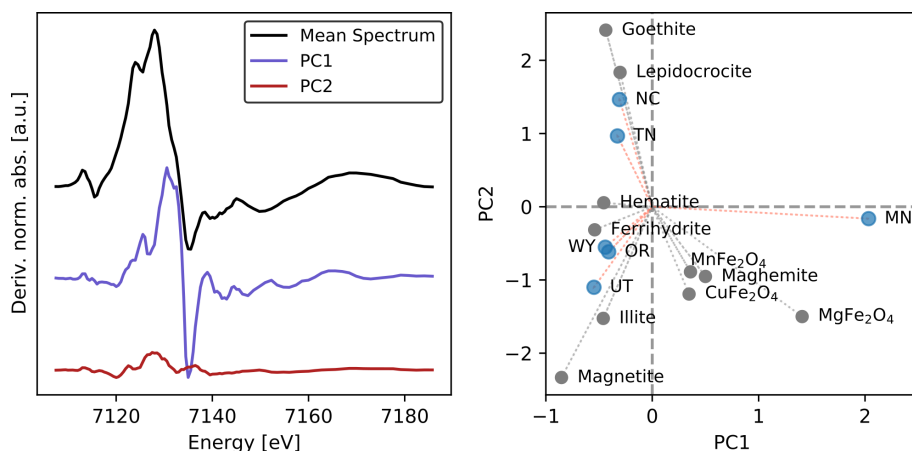


Figure 4: Principal components analysis of Fe K-edge first-derivative XANES spectra for drinking water treatment residuals. The left subplot visualizes the principal components. First, the mean first-derivative XANES spectrum calculated from all the DWTR sample spectra is plotted. Principal components are calculated based on the distance of the samples from the mean across each spectrum. The components plotted in the left subplot are therefore added or subtracted from the mean spectrum to approximately recreate the sample spectra. PC1 and PC2 are scaled based on the variance they account for within the Fe K-edge DWTR spectra (85% and 12%, respectively). The right subplot projects the DWTR samples along with selected standards on the first two principal components. Here, it is clear that most of the variance is driven by the MN sample. This is reflected in the shape of PC1, which shows the shoulder and small oscillations in the first-derivative XANES that distinguished MN from the other samples. In the projection of standards, common ferric (or mixed-valence iron) minerals do not recreate these features. However, a number of spinel ferrite minerals, including maghemite, manganese ferrite (jacobsite), copper ferrite (cuprospinel), and magnesium ferrite (magnesioferrite) do.

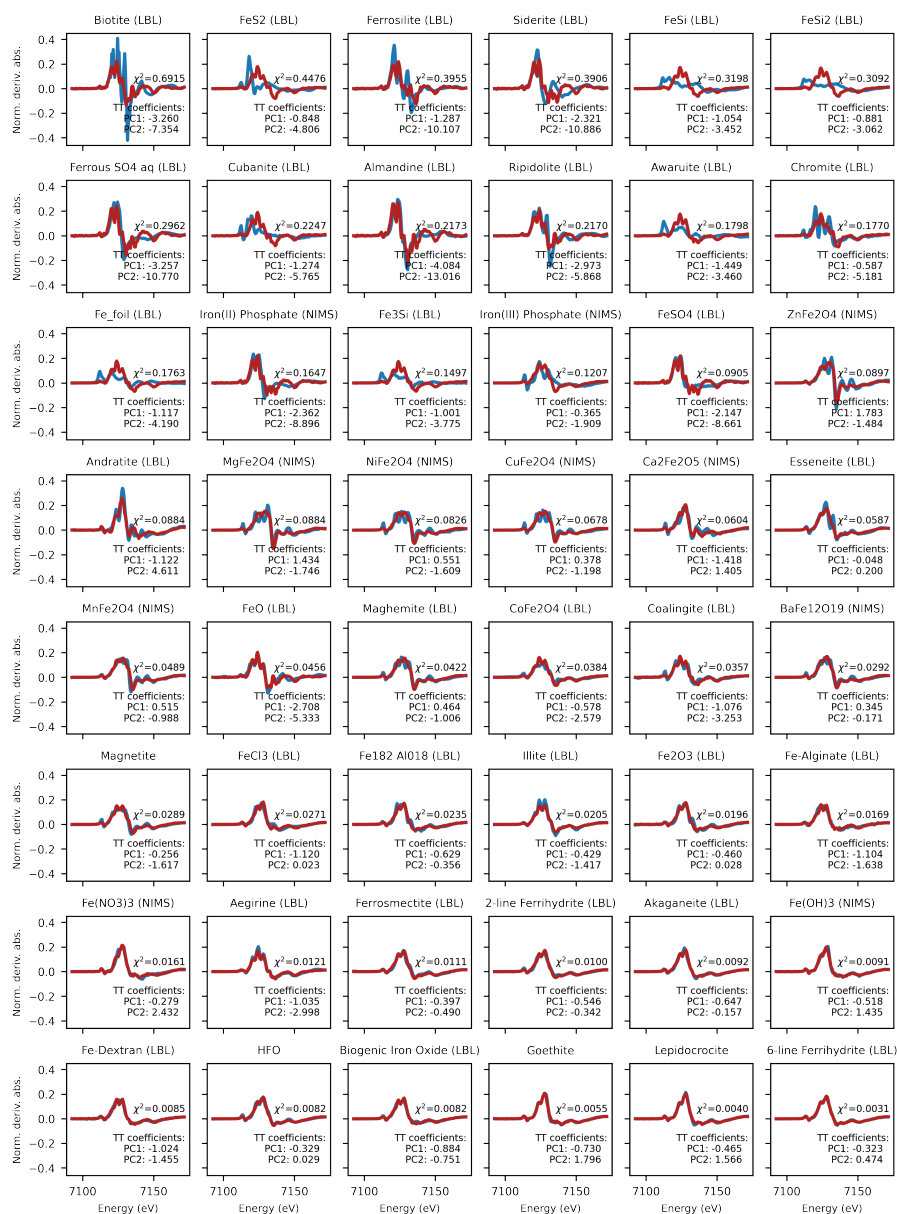


Figure 5: Target transformations of first-derivative Fe K-edge XANES standard spectra based on principal components calculated from DWTRs. “LBL”³ and “NIMS”^{4,5} identify databases from which certain spectra were acquired.

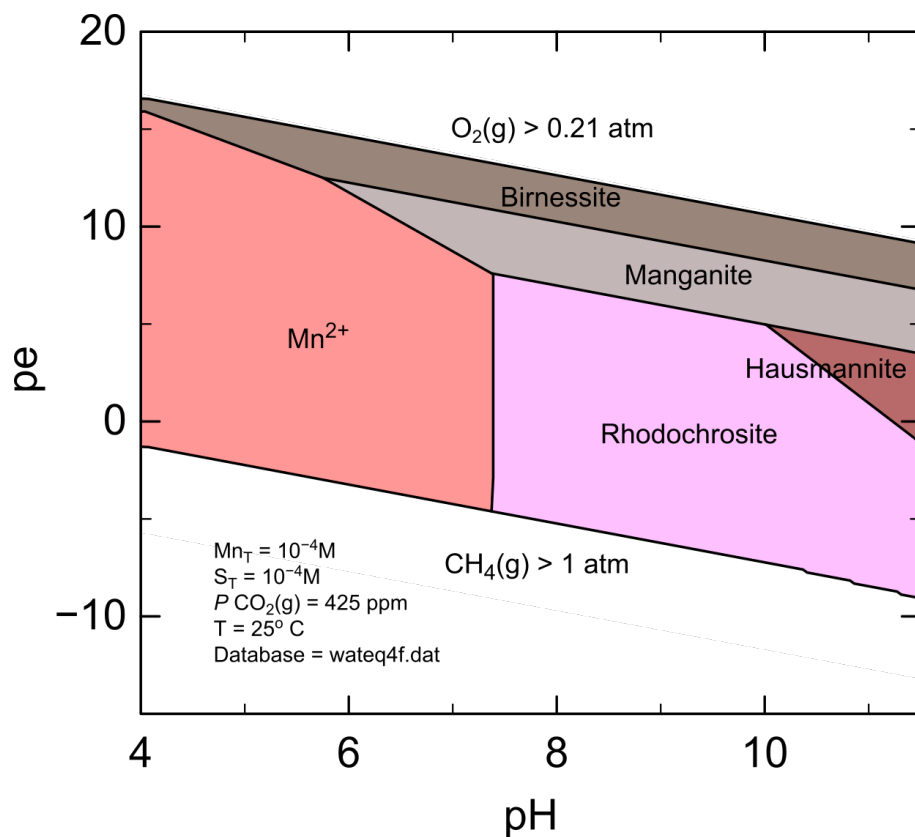


Figure 6: Pourbaix diagram showing stable manganese phases in solution. Calculations were performed and plotted using Phreeplot software¹ and the WATEQ4F thermodynamic database². Calculations assume 100 μM total Mn, 100 μM total S, equilibrium with 425 ppm atmospheric CO_2 , and 25°C temperature. Pyrolusite (MnO_2) and bixbyite (Mn_2O_3) were not included in calculations to emphasize manganese species that are more easily formed through surface water processes.

References

- [1] D. Kinniburgh and D. Cooper, *Phreeplot: Creating Graphical Output with Phreeqc*, 2011.
- [2] J. W. Ball, D. K. Nordstrom and D. W. Zachmann, *Wateq4f- a Personal Computer Fortran Translation of the Geochemical Model Wateq2 with Revised Data Base*, U.S. Geological Survey Report 2331-1258, 1987.
- [3] S. Fakra, *Xas Databases*, 2010, <http://xraysweb.lbl.gov/uxas/databases/overview.htm>.
- [4] M. Tanifuji, A. Matsuda and H. Yoshikawa, 2019 8th International Congress on Advanced Applied Informatics (IIAI-AAI), 2019, pp. 1021–1022.
- [5] M. Ishii, H. Nagao, K. Tanabe, A. Matsuda and H. Yoshikawa, *MDR XAFS DB*, 2021, Materials Data Repository, National Institute for Materials Science.